HHS Public Access

Author manuscript

J Vasc Res. Author manuscript; available in PMC 2023 June 27.

Published in final edited form as:

J Vasc Res. 2022 ; 59(5): 275–287. doi:10.1159/000525259.

Apolipoprotein A-I inhibits transendothelial transport of apolipoprotein B-carrying lipoproteins and enhances its associated high-density lipoprotein formation

Zhongmao Guo,

Ningya Zhang,

Hong Yang

Department of Microbiology, Immunology and Physiology, Meharry Medical College, Nashville, TN 37208, USA

Abstract

Caveolae-located scavenger receptor type B class I (SR-BI) and activin receptor-like kinase-1 (ALK1) are involved in transendothelial transport of apolipoprotein B-carrying lipoproteins (apoB-LPs). Transport of apoB-LPs though mouse aortic endothelial cells (MAECs) is associated with apoE-carrying high-density lipoprotein (HDL)-like particle formation and apoAI induces raft-located proteins to shift to non-raft membranes by upregulation of ATP-binding cassette transporter A1 (ABCA1). To investigate apoAI's effect on transendothelial transport of apoB-LPs, MAECs and human coronary artery endothelial cells (HCAECs) were treated with apoB-LPs ± apoAI. Our data demonstrated that apoAI neither altered SR-BI and ALK1 expression, nor affected apoB-LP binding to MAECs. ApoAI inhibited MAEC uptake, transcellular transport, and intracellular accumulation of apoB-LPs, and accelerated their resecretion in MAECs. ApoAI enhanced transendothelial apoB-LP transport-associated HDL-like particle formation, upregulated ABCA1 expression, shifted SR-BI and ALK1 to the non-raft membrane in MAECs, and inhibited transcellular transport of apoB-LPs and enhanced associated HDL-like particle formation in HCAECs. ABCA1 knockdown attenuated apoAI-induced membrane SR-BI and ALK1 relocation and diminished apoAI's effect on transendothelial apoB-LP transport and HDL-like particle formation in MAECs. This suggests that upregulation of ABCA1 expression is a mechanism whereby apoAI provokes caveolae-located receptor relocation, inhibits transendothelial apoB-LP transport, and promotes associated HDL-like particle formation.

Corresponding Author: Hong Yang, Department of Microbiology, Immunology and Physiology, Meharry Medical College, 1005 Dr. T.B. Todd Jr. Blvd, Nashville, TN 37208, USA, Tel: 615-327-5772, hyang@mmc.edu.

Author Contributions

Zhongmao Guo and Hong Yang designed the experiments, analyzed the data, wrote the manuscript, and acquired funding for the experiments. Ningya Zhang performed the experiments and was involved in data analysis.

Conflicts of interest

The authors have no conflicts to disclose.

Statement of Ethics

This research did not involve human subjects or animal models. Mouse endothelial cells were purchased from Cell Biologics, Inc. (Chicago, IL).

Keywords

endothelial cell; apolipoprotein A-I; transendothelial lipoprotein transport; membrane microdomain reorganization; high-density lipoprotein

Introduction

Passage of plasma apolipoprotein (apo) B-carrying lipoproteins (apoB-LPs), including triglyceride-rich lipoproteins (TRLs) and low-density lipoproteins (LDLs), to the subendothelial intima is an initial step of atherogenesis. It has been established that these lipoproteins can pass over the monolayer endothelium via paracellular and transcellular pathways [1]. The transcellular transport includes at least four steps: (1) receptor binding; (2) endocytosis; (3) intracellular vesicle trafficking; and (4) exocytosis. It has been reported that endothelial cell endocytosis and transport of LDLs is mediated by a caveolae-dependent pathway. Caveolae are a subset of lipid rafts that contain caveolins and specific receptors involved in endocytosis. It also has been reported that knockout of caveolin-1 diminished LDL endocytosis in cultured endothelial cells [2], suppressed LDL transport to the mouse arterial wall [3], and inhibited atherosclerosis in mouse models [4]. In addition, underexpression of caveolae-located receptors scavenger receptor type B class I (SR-BI) [5] or activin receptor-like kinase-1 (ALK1) [6] has been shown to inhibit LDL endocytosis in cultured endothelial cells. Accordingly, endothelial uptake of LDL is thought to be via SR-BI- and/or ALK1-mediated endocytosis that uses caveolar vesicles to bring LDLs into cells. In many cell types, such as hepatocytes and macrophages, the caveolar endocytic vesicles deliver their contents to sorting endosomes [7] where internalized cargos are allotted to either lysosomes for degradation or recycling endosomes for re-secretion. We previously reported that the apoB-LP-associated apoB and apoE proteins, which were internalized into mouse aortic endothelial cells (MAECs) or had passed through the MAEC monolayer, exhibited normal sizes as those in native apoB-LPs [8]. This is consistent with a report showing that the LDL particles endocytosed from the apical (AP) side of cultured endothelial cells were not delivered to lysosomes but were transported to the basolateral (BL) side as holoparticles [5].

Our previous studies demonstrated that TRLs and LDLs share the same pathway for transport through mouse aortic endothelial cells (MAECs) [8]. The apoB-LPs that had passed through the MAEC monolayer were disintegrated into two types of particles: apoE-carrying high-density particles and apoB-/apoE-carrying low-density particles [8]. These suggest that a portion of apoE and lipids dissociate from apoB-LPs and exit endothelial cells as apoE-carrying high-density lipoprotein (HDL)-like particles. Dissociation of apoE from endocytosed apoB-LPs is not cell-specific, as it has been seen in other cell types such as macrophages and hepatocytes [9, 10]. The re-secreted apoE either is floated with lipids or presented in a relatively lipid-poor state [11]. It has been shown that combinational treatment of hepatocytes with apoB-LPs and apoAI promotes apoE-carrying HDL-like particle secretion [12, 13]. ApoAI is the major protein component of HDL. However, lipid-free/lipid poor apoAI has been detected in the plasma and the arterial intimal fluid [14, 15]. It has been suggested that lipid-free/lipid-poor apoAI is generated, at least partially, by

HDL delipidation in the blood compartment, and then transported to the intimal fluid by endothelial cells [16]. To our knowledge, the effect of apoAI on apoE-carrying HDL-like particle formation in endothelial cells has never been reported.

Another function of apoAI is to upregulate the expression of ATP-binding cassette transporter A1 (ABCA1). It has been reported that binding of apoAI to cell surface ABCA1 triggers several signaling pathways [17-19]. Among these pathways, activation of the cyclic adenosine 3,5-monophosphate (AMP)–protein kinase A (PKA) pathway has been shown to increase ABCA1 stability [20] and upregulate its expression at the transcription level [17]. The best-known activity of ABCA1 is its transport of phospholipids and unesterified cholesterol to apoAI, forming nascent HDL particles. Additionally, ABCA1 is able to regulate the organization of membrane microdomains by redistribution of raft lipids and proteins to the non-raft domains [21, 22]. We recently reported that treatment of MAECs with apoAI increased the messenger ribonucleic acid (mRNA) and protein levels of ABCA1, and induced relocation of caveolin-1 and cholesterol from the raft to non-raft membrane [23]. Knockdown of ABCA1 diminished apoAI-induced redistribution of caveolin-1 and cholesterol among membrane microdomains [23].

The current report, for the first time, demonstrates that upregulation of ABCA1 is a mechanism by which apoAI induces caveolae-located receptor relocation, inhibits the transport of apoB-LPs through the endothelial cell monolayer, and enhances endothelial apoB-LP transport-associated HDL-like particle formation.

Materials and Methods

Chemicals and reagents

Human apoAI and apoE3 were purchased from Athens Research and Technology (Athens, GA) and Leinco Technologies (St. Louis, MO), respectively. Transwell™ polycarbonate membrane cell culture inserts (07200156 and 07200170); Pierce™ Iodination Beads (PI28665); Zeba™ Spin Desalting Columns, 7K MWCO (#89891); OptiMEM™ Reduced Serum Medium; M-PER™ Mammalian Protein Extraction Reagent; polyvinylidene fluoride (PVDF) membranes; and ECL plus chemiluminescence reagent were purchased from ThermoFisher Scientific (Waltham, MA). [1,2-^{3}H(N)]-cholesterol (^{3}H-Ch) and 125-Iodine (^{125}I) were obtained from American Radiolabeled Chemicals (St. Louis, MO) and PerkinElmer, Inc. (Waltham, MA), respectively. Freshly collected human blood was obtained from BiolVT (Fredrick, MD). Antibodies against caveolin-1, clathrin heavy chain 1 (CLTC), ALK1, ABCA1, apoE, apoB, and β-actin, as well as scrambled small interfering RNA (siRNA) and ABCA1 siRNAs (ABCsi), were purchased from Santa Cruz Biotechnology, Inc. (Santa Cruz, CA). OptiPrep™ Density Gradient Medium was obtained from Sigma-Aldrich (St. Louis, MO). Thiobarbituric acid-reacting substances (TBARS) assay kit was obtained from ZeptoMetrix Co. (Buffalo, NY). MAECs and the endothelium medium with growth factor supplement kit were obtained from Cell Biologics, Inc. (Chicago, IL). Human primary coronary artery endothelial cells (HCAECs) and vascular cell basal medium were purchased from American Type Culture Collection (ATCC) (Manassas, VA). The sixth to ninth passages of cells were used in the current study.

Isolation of radiolabeled and unlabeled lipoproteins

ApoB-LPs were radiolabeled and isolated as described previously [8]. Briefly, 300 μCi of ^{3}H-Ch was incubated with 50 ml human plasma containing 50 μM butylated hydroxytoluene at 37°C for 18 h. The unassociated ^{3}H-Ch was removed by incubation with equal volume of autologous packed erythrocytes at 37°C for 2 h. The erythrocytes were removed by centrifugation at 16,000 g x 5 min at 4°C. Radiolabeled and unlabeled apoB-LPs (d < 1.063) were isolated by potassium bromide (KBr) density gradient ultracentrifugation. Lipoproteins labeled in this manner contain both esterified and unesterified ^{3}H-Ch [24]. For preparation of ^{125}I-apoB-LPs, human apoE was labeled with ^{125}I using Pierce™ Iodination Beads, per manufacturer's instructions. Free iodine was removed from the labeled apoE by passage through Zeba™ Spin Desalting Columns. The eluent was centrifuged at 16,000 g x 10 min at 4°C, and the pellet was discarded. After incubation with human plasma for 3 h at 37°C, ^{125}I-apoB-LPs were isolated by KBr density gradient ultracentrifugation at d < 1.063 g/ml. The oxidized level of lipoproteins was determined using a TBARS assay kit. The unlabeled and ^{25}I-labeled apoB-LPs used in this study contained 0.5-0.8 and 0.7-1.0 nmol/of TBARS per mg proteins. These are comparable to the oxidative levels of the native apoB-LPs, as previously reported [25, 26].

Determination of endothelial cell binding of apoB-LPs

MAECs were seeded in a 12-Well plate in endothelium medium with growth factor supplement to confluence, unless otherwise stated. For determination of dose-dependent binding of apoB-LPs, the medium was replaced with 1 ml of OptiMEM™ medium. The plate was incubated on ice for 30 min, and then 0 μg/ml to 60 μg/ml of ^{125}I-labeled apoB-LPs was added into the medium and incubated on ice for 30 min. For determination of the effect of apoAI on apoB-LP binding, the medium was replaced with 1 ml of OptiMEM™ medium supplemented with 0 μg/ml to 30 μg/ml of apoAI. The plate was incubated sequentially at 37°C for 4 h and on ice for 30 min, and then 20 μg/ml of ^{125}I-labeled apoB-LPs was added into the medium and incubated on ice for 30 min. The cells were washed twice with ice-cold phosphate-buffered saline (PBS) and lysed with 0.5 M NaOH. An aliquot (10 μl) of lysate was used for measurement of cell protein concentration, and the remaining lysate was used to determine radioactivity using a universal γ-counter (1282 Compugamma, PerkinElmer Life & Analytic Science, Shelton, CT). The radioactivity bound to endothelial cells was normalized as disintegrations per minute (DPM) / mg cell proteins.

Determination of endothelial cell uptake, transcellular transport, accumulation, and resecretion of apoB-LPs

MAECs were seeded in 0.4 μm Transwell™ inserts and cultured in 6-Well plates in endothelium medium with growth factor supplement to confluence. The AP medium was replaced with OptiMEM™ medium supplemented with 20 μg/ml of ^{125}I-labeled apoB-LPs ± 20 μg/ml of apoAI, while the BL side was replaced with OptiMEM™ medium alone. After incubation at 37°C for 24 h, the BL medium was collected, and the MAEC monolayer was washed twice with 100 units heparin and then lysed in 0.5 N NaOH. The amount of apoB-LPs transported through the MAEC monolayer and accumulated in MAECs was determined by radioactivity in the BL medium and cell lysate, respectively. The amount of

apoB-LPs taken up by MAECs was the sum of radioactivity associated with and transported by the cells and was calculated as: uptake = accumulated + transport. In the experiments for determination of ^{125}I-apoE re-secretion, the MAEC monolayer was washed thrice with a low ionic strength solution of 0.2x PBS supplemented with 300 mM glycine and 5% bovine serum albumin to remove the surface-bound materials. Fresh OptiMEM™ medium was then added into both the AP and BL chambers and incubated for another 24 h. The amount of apoE secreted by MAECs was determined by the sum of radioactivity in the AP and BL media.

Determination of cholesterol and apolipoprotein distributions in lipoproteins

To study the effect of transendothelial transport on the distribution of cholesterol in lipoproteins, the AP side of the MAEC monolayer and the HCAEC monolayer were incubated with OptiMEM™ medium supplemented with 20 μg/ml of ^{3}H-Ch-labeled apoB-LPs ± 20 μg/ml of unlabeled apoAI. To study the effect of transendothelial transport on the distribution of apolipoproteins in lipoproteins, the AP side of the MAEC monolayer was incubated with OptiMEM™ medium supplemented with 20 μg/ml unlabeled apoB-LPs ± 20 μg/ml of unlabeled apoAI, or 0.2 μg/ml of ^{125}I-apoAI ± 20 μg/ml unlabeled apoB-LPs. In all these experiments, the BL side was incubated with OptiMEM™ medium alone. After 24 h incubation, the BL medium was collected and centrifuged at 16,000 x *g* for 10 min. As controls, 20 μg/ml of ^{3}H-Ch-labeled apoB-LPs or 20 μg/ml unlabeled apoB-LPs was incubated with OptiMEM™ medium in the absence of cells at 37°C for 24 h. The BL medium supernatants and the cell-untreated lipoproteins, or apoAI medium, were subjected to discontinuous NaCl/KBr density gradient ultracentrifugation [8, 27]. In brief, the medium samples were adjusted to 1.21 g/ml by addition of KBr. The discontinuous density gradient was constructed by sequentially layering the following solutions into a centrifugation tube: (1) 2 ml of 1.35 g/ml KBr; (2) 3 ml of 1.21 g/ml KBr (medium samples); (3) 3 ml of 1.063 g/ml KBr; (4) 2 ml of 1.019 g/ml KBr; and (5) 2 ml of 1.006 g/ml NaCl [27]. The constructed gradients were centrifuged at 40,000 x g at 20°C for 24 h using a SW-41 rotor, and twenty fractions (0.57 ml/fraction) were collected for radioactivity and immunoblotting analyses. We previously demonstrated that the density of the ninth fraction is ~1.063 g/ml. Thus, we designated fractions one through nine and fractions ten through twenty as low-density fractions (LDFs) and high-density fractions (HDFs), respectively [8].

In experiments in which radiolabeled apoB-LPs or apoAI was used, radioactivity in each fraction was counted separately for plotting the density distribution curve of cholesterol and apoAI. The amount of cholesterol and apoAI distributed in LDFs and HDFs was determined by the sum of radioactivity in fractions one through nine and fractions ten through twenty, respectively. In experiments in which only unlabeled apoB-LPs and apoAI were used, solutions from fractions one through nine and those from fractions ten through twenty were pooled separately for Western blot (WB) analysis of apoB and apoE.

Separation of membrane raft and non-raft membranes

The membrane lipid rafts were separated from non-raft membrane using a detergent-free method [8, 28]. Briefly, MAECs were washed and scraped into a base buffer (20 mM Tris HCl, pH 7.8, 250 mM sucrose) freshly supplemented with 1 mM $CaCl_2$ and 1 mM $MgCl_2$.

After pelleting by centrifugation at 1,000 x g for 5 min, cells were resuspended in 1 ml of homogenization buffer containing 20 mM Tris HCl, 250 mM sucrose, 1 mM $CaCl_2$, 1 mM $MgCl_2$, and 10 μl/ml protease inhibitor cocktail and homogenized by passage through a 22 g × 3" needle 25 times. The homogenate was centrifuged at 1,000 x g for 10 min. The resulting postnuclear supernatant was collected, the pellet was resuspended, and the homogenization procedures were repeated one time. The postnuclear supernatants collected following the two rounds of homogenations were combined and mixed with an equal volume of base buffer containing 50% OptiPrep™, which yielded 25% in OptiPrep™. Four ml of the resulting mixture was placed in the bottom of a 12-ml centrifuge tube. A 6-ml gradient of 0% to 20% OptiPrep™ in base buffer was poured on top of the mixture. Gradients were centrifuged using a SW-41 rotor in a Beckman ultracentrifuge for 90 min at 52,000 *x* g. Two fractions were collected from the top to the bottom of the centrifuged gradient for WB analysis. The upper and lower fractions contained 6 ml and 4 ml of the gradient, respectively. We previously demonstrated that the non-raft mark protein CLTC exclusively distributes in 4 ml of the lower fraction [28]. Therefore, we designated the upper and lower fractions of this centrifuged gradient as raft and non-raft fractions, respectively.

siRNA knockdown of ABCA1

MAECs were transfected with specific siRNAs against ABCA1 or scrambled control siRNAs (Ctrlsi) according to the manufacturer's instructions. After 6 h, cells were replenished with fresh endothelium medium plus growth factor supplement and cultured for an additional 24 h. These transfection procedures were repeated one time [29]. The knockdown efficiency induced by siRNA was confirmed by detection of ABCA1 proteins using WB analysis.

Quantitative real-time reverse transcription (RT)-polymerase chain reaction (PCR) assay

Total RNA was extracted from MAECs using Trizol reagent (ThermoFisher Scientific), treated with DNAse I, and subjected to RT using the Applied Biosystems™ high-capacity cDNA reverse transcription kit (ThermoFisher Scientific). The resulting cDNAs were subjected to quantitative real-time RT-PCR with the following primers: ABCA1 forward (4'-GCTACCCACCCTACGAACAA-3), reverse (5'-GGAGTTGGATAACGGAAGCA-3'); and glyceraldehyde 3-phosphate dehydrogenase (GAPDH) forward (5'-GAGCCAAAAGGGTCATCATC-3'), reverse (5'-TAAGCAGTTGGTGGTGCAGG-3'). The expression levels of ABCA1 mRNA were normalized to GAPDH mRNA.

Western blot analysis

Proteins in the gradient fractions collected from the NaCl/KBr and the OptiPrep™ density gradient ultracentrifugation were precipitated by 75% methanol. For measurement of the proteins in the whole cell, MAECs were lysed using M-PER™ Mammalian Protein Extraction Reagent. An aliquot of protein extracts was used for measurement of cell protein concentration, and the remaining protein preparations were resolved on 10% SDS-PAGE gels. Proteins were transferred to a PVDF membrane. After blocking with 3% fat-free milk, the membranes were incubated with antibodies against apoB, apoE, ABCA1, SR-BI, ALK1, CLTC, or β-actin. Immunoreactive bands were visualized using

ECL plus chemiluminescence reagent (GE Healthcare–Amersham) and analyzed with a GS-700 Imaging Densitometer (Bio-Rad Laboratories, Hercules, CA). The level of the studied proteins was expressed as immunoreactive intensity (arbitrary units) / mg endothelial cell proteins.

Statistical analysis

Data are reported as the mean ± SEM, and data distribution was examined by the Shapiro-Wilk normality test. Differences among groups were analyzed by Student's unpaired *t*-test (for two groups) and one-way analysis of variance (for more than two groups), followed by Tukey's post-hoc test. Statistical significance was considered when P was less than 0.05. GraphPad software was used for statistical analysis.

Results

Effect of apoAI on MAEC binding, uptake, transcellular transport, and re-secretion of apoB-LPs

To study apoB-LP binding, MAECs were incubated with various concentrations of ^{125}I-apoB-LPs on ice for 4 h. As seen in Figure 1A, cell-bound radioactivity increased with the concentration of ^{125}I-apoB-LPs in the culture medium, plateauing at a concentration of 40 μg/ml and remaining constant at concentrations up to 60 μg/ml. To determine the effect of apoAI on apoB-LP binding, MAECs were treated with various concentrations of apoAI at 37°C for 4 h and then incubated with 20 μg/ml of ^{125}I-apoB-LPs on ice for 30 min. The data in Figure 1B show that pretreatment of MAECs with apoAI did not significantly alter the amount of ^{125}I-apoB-LP bound to MAECs.

We previously reported that ~6% to 8% of ^{125}I-labeled TRLs, IDLs, and LDLs were transported through the MAEC monolayer during 24 h at 37°C and that the transport of these radiolabeled apoB-LPs could be suppressed by their unlabeled counterparts [8]. To study the effect of apoAI on MAEC uptake, accumulation, transcellular transport, and re-secretion of apoB-LPs, we incubated the AP side of the MAEC monolayer with 20 μg/ml of ^{125}I-apoB-LPs (167,000 DPM) in the absence or presence of 20 μg/ml of apoAI. As Figure 1 shows, in the absence of apoAI, ~9,700 DPM of radioactivity (~5.8% of ^{125}I-apoB-LPs) was transported from the AP chamber to the BL chamber (Fig. 1C); ~3,500 DPM of radioactivity (2.1% of apoB-LPs) was accumulated in MAECs (Fig. 1D). The addition of apoAI to the AP medium reduced the amount of apoB-LPs accumulated in MAECs and those transported to the BL medium (~5,700 DPM and 1,300 DPM of radioactivity presented in the BL medium and MAECs, respectively (Figs. 1C-1D). In this study, MAEC uptake of lipoproteins was determined by the total ^{125}I-apoB-LPs accumulated in cells and transported to the BL medium. As the data in Figure 1E show, apoAI significantly diminished MAEC uptake of apoB-LPs: ~13,200 DPM of radioactivity was taken up by MAECs treated with apoB-LPs alone, and only ~7,000 DPM of radioactivity was taken up by cells treated with both apoB-LPs and apoAI.

To investigate the mechanism underlying the inhibitory effect of apoAI on cellular apoB-LP accumulation, we determined the re-secretion of lipoproteins from MAECs. As Figure 1F

shows, the re-secreted radioactivity from MAECs treated with both apoB-LPs and apoAI was ~44% more compared with those treated with apoB-LPs alone. ApoAI treatment significantly increased the re-secretion of apoB-LPs from MAECs.

Effect of apoAI on formation of apoE-carrying HDL-like particles in endothelial cells

The AP-to-BL transendothelial transport of apoB-LPs has been shown to be associated with the generation of apoE-carrying HDL-like particles [8]. Herein, we studied the effect of apoAI on the density redistribution of apoB-LP-derived cholesterol in the BL medium of the MAEC monolayer. As the radioactivity distribution curve in Figure 2A illustrates, the ^{3}H-Ch of cell-untreated apoB-LPs distributes primarily in fractions one through nine: the LDFs. Incubation of the AP side of the MAEC monolayer with 20 μg/ml (35,000 DPM) of ^{3}H-Ch-labeled apoB-LPs induces a portion of ^{3}H-Ch transported to the BL medium, and the transported ^{3}H-Ch distributes in both LDFs and HDFs (Fig. 2A). As the data in Figures 2B-2C show, ~1,700 DPM of radioactivity was transported through the vehicle-treated MAEC monolayer in 24 h and ~44% of radioactivity was distributed in the HDFs. Treatment of the MAEC monolayer with apoAI inhibits transendothelial transport of ^{3}H-Ch and enhances its redistribution from the LDFs to HDFs. Specifically, only ~1,100 DPM of radioactivity was transported through the apoAI-treated MAEC monolayer within 24 h (Fig. 2B), and ~69% of transported radioactivity presented in the HDFs (Fig. 2C). The difference of these measurements between the vehicle- and apoAI-treated cells was statistically significant (Figs 2B-2C).

We also investigated the effect of apoAI on transport of apoB-LPs through the HCAEC monolayer and its associated apoE-carrying HDL-like particle formation. As seen in Figures 2B and 2C, ~1,900 DPM and 1,300 DPM of radioactivity were transported through the HCAEC monolayer treated with vehicle medium or apoAI in 24 h, respectively (Fig. 2B), and ~37% and ~62% of transported radioactivity were found in the HDFs of the BL medium of the vehicle-treated or apoAI-treated HCAEC monolayer, respectively (Fig. 2C). The transported radioactivity is significantly less, and the HD/total radioactivity ratio is significantly greater in the BL medium of the apoAI-treated HCAEC monolayers compared to those in the BL medium of the HCAEC monolayers treated with vehicle medium. There is no significant difference in the transported radioactivity nor the HD/total radioactivity ratio between the HCAEC and the MAEC monolayers.

ApoAI has shown the ability to pass through the endothelial monolayer. ApoAI apically endocytosed by endothelial cells could be re-secreted basolaterally [30]. To determine the density distribution of the transendothelially transported apoAI, the AP side of the MAEC monolayer was incubated with ^{125}I-apoAI in the presence or absence of unlabeled apoB-LPs. As the radioactivity distribution curve in Figure 2D illustrates, in the absence of apoB-LPs, ~90% of radioactivity in the BL medium distributes in fraction twenty, which has a density of 1.25. This suggests that most of the transported ^{125}I-apoAI existed in a lipid-free form. In contrast, in the experiment where apoB-LPs were present in the AP medium, radioactivity in the BL medium exhibits multiple peaks in the HDFs, meaning most of the ^{125}I-apoAI that had passed through the MAEC monolayer distributes between densities of

1.063 and 1.21. This suggests that the apoAI passed through the MAEC monolayer was lipidated and exists in the HDL-sized particles.

Effect of apoAI on redistribution of apoE in transendothelially transported lipoproteins

Transport of apoB-LPs through MAECs has been shown to induce a shift of their associated apoE to HDL-like particles, but no effect on the density distribution of their associated apoB [8]. To determine whether apoAI affects the transendothelial transport of apoB-LP-associated apoB and apoE and the density distribution of these apolipoproteins, we incubated the AP side of the MAEC monolayer with apoB-LPs ± apoAI, and determined the protein level and the density distribution of apoB and apoE in the BL medium. The data in Figures 3A-3B show that apoAI inhibited the transendothelial transport of apoB-LP-associated apoB and apoE. Specifically, the protein level of apoB and apoE in the BL medium of the apoAI-treated MAEC monolayer was ~36% and ~22% less, respectively, compared with those in the BL medium of the vehicle-treated MAEC monolayer (Fig 3B). The WB images in Figure 3A illustrate that apoB is detectable only in the LDF, but not in the HDF, either in the cell-untreated apoB-LPs or in the BL medium of the MAEC monolayer treated with apoB-LPs ± apoAI. This suggests that incubation of apoB-LPs with the MAEC monolayer either in the presence or absence of apoAI does not induce apoB redistribution among the density fractions. The images in Figure 3A also show that apoE in cell-untreated apoB-LPs is barely detectable in the HD fraction, the incubation of apoB-LPs with the MAEC monolayer resulted in apoE shift from the LDF to HDF, and the addition of apoAI into the AP medium further augmented the redistribution of apoE to the HDF. Specifically, the HDF/total apoE ratio was ~48% and ~72% in the BL medium of the MAEC monolayer treated with apoB-LPs in the presence of vehicle medium or apoAI, respectively (Fig. 3C). The difference between the apoAI-treated and vehicle-treated MAEC monolayers was statistically significant.

Effect of apoAI treatment and ABCA1 knockdown on membrane distribution of SR-BI, ALK1, and CLTC

The data in Figure 4 show that apoAI upregulated ABCA1 expression in MAECs. Specifically, the mRNA and protein levels of ABCA1 were ~36% and ~41% higher, respectively, in apoAI-treated MAECs than in those treated with vehicle medium (Fig. 4A-4C). In contrast, the WB images in Figure 4B show that apoAI did not alter the protein level of β-actin in MAECs.

We recently reported that apoAI is able to induce caveolin-1 shift from the raft to non-raft membrane via an ABCA1-dependent manner [23]. The present study examined the effect of apoAI treatment and ABCA1 knockdown on the expression and membrane distribution of the caveolae-associated receptors SR-BI and ALK1, as well as the non-raft protein CLTC in MAECs. As shown in Figures 4D and 4E, apoAI treatment upregulated ABCA1 expression in MAECs transfected with scrambled Ctrlsi or ABCsi. Transfection of ABCsi diminished basal and apoAI-induced ABCA1 expression. Specifically, the ABCA1 protein levels in scrambled siRNA-transfected MAECs and ABCsi-transfected cells under apoAI treatment conditions were ~40% and ~47% higher, respectively, than those under vehicle treatment conditions (Fig. 4E). The ABCA1 protein levels in ABCsi-transfected MAECs under the

vehicle and apoAI treatment conditions were ~36% and 28% lower, respectively, compared with those in the scrambled siRNA-transfected cells with vehicle and apoAI treatments (Fig. 4E). The images in Figure 4D illustrate that apoAI treatment and ABCA1 knockdown did not affect the expression of SR-BI, ALK1, CLTC or β-actin in MAECs. The protein level of SR-BI, ALK1 and CLTC in cells transfected with ABCsi or scrambled siRNAs and treated with or without apoAI is comparable (Fig. 4E).

Figure 4F illustrates typical immunoblot images of SR-BI, ALK1, and CLTC in the raft and non-raft membrane fractions. The data in Figure 4G show that the percentage of SR-BI in the raft membrane fraction was reduced by apoAI treatment. Specifically, ~56% of SR-BI is located in the raft membrane of vehicle-treated, scrambled siRNA-transfected MAECs. The remaining SR-BI distributes in the non-raft fraction, co-existing with CLTC. In contrast, only ~25% of SR-BI is located in the raft membrane of apoAI-treated, scrambled siRNA-transfected MAECs, which was significantly less compared with that in the vehicle-treated cells. Further, siRNA knockdown of ABCA1 augmented the percentage of SR-BI in the raft membrane fraction. Approximately 69% and 49% of SR-BI distributes in the raft membrane of the ABCsi-transfected cells treated with vehicle medium or apoAI, respectively (Fig. 4G). These values are significantly greater than those in the scrambled siRNA-transfected cells treated with or without apoAI, respectively.

The membrane microdomain redistribution induced by apoAI treatment and ABCA1 knockdown also was observed in ALK1. Specifically, ~60% and 35% of ALK1 was found in the raft membrane fraction of the scrambled Ctrlsi-transfected MAECs treated with the vehicle medium and apoAI, respectively. In contrast, ~77% and 52% of ALK1 was found in the raft membrane of the ABCsi-transfected cells under the vehicle and apoAI treatment conditions, respectively. The difference of the percentage of raft ALK1 between vehicle and apoAI-treated cells, and the difference between Ctrlsi and ABCsi-transfected cells, is statistically significant.

The data in Figure 4F also show that apoAI treatment and ABCA1 knockdown did not alter membrane CLTC distribution. This protein distributes exclusively in the non-raft fraction, whether the cells were transfected with scrambled or ABCA1-specific siRNA, or treated with vehicle medium or apoAI.

Effect of ABCA1 knockdown on transendothelial apoB-LP transport and its associated HDL-like particle formation

The AP side of the siRNA-transfected MAEC monolayer was treated with ^{3}H-Ch-apoB-LPs (35,000 DPM) ± apoAI for 24 h. The transendothelially transported apoB-LPs and associated HDL-like particle formation were determined by radioactivity in the BL medium. The radioactivity density distribution curves in Figures 5A-5B show that the transported ^{3}H-Ch distributes in both LDFs and HDFs of the BL medium, regardless of whether the MAEC monolayer was transfected with scrambled Ctrlsi (Fig. 5A) or ABCsi (Fig. 5B), or was treated with or without apoAI. However, the transported amount and the density distribution of ^{3}H-Ch in the BL medium vary among the MAEC monolayers subjected to particular treatments (Figs. 5C and 5D). Specifically, ~1,900 DPM and 1,300 DPM (~5.4% and 3.7%) of radioactivity loaded to the AP chamber were transported through

the Ctrlsi-transfected MAEC monolayer under vehicle and apoAI treatment conditions, respectively (Fig. 5C). In contrast, ~2,400 DPM and 2,100 DPM (~6.9% and 6%) of radioactivity were transported through the ABCsi-transfected MAEC monolayer under vehicle and apoAI treatment conditions, respectively (Fig. 5C). ApoAI treatment reduced the transport of ^{3}H-Ch-apoB-LPs through the Ctrlsi-transfected MAEC monolayers, but did not significantly affect the transport of ^{3}H-Ch-apoB-LPs through the ABCsi-transfected MAEC monolayer. Knockdown of ABCA1 significantly elevated the transport of ^{3}H-Ch through the monolayers treated ± apoAI.

Figure 5D shows that ~37% of the ^{3}H-Ch that passed through the vehicle-treated, Ctrlsi-transfected MAEC monolayer distributes in the HDFs of the BL medium. Incubation of this MAEC monolayer with apoAI elevated the percentage of ^{3}H-Ch that shifted to the HDFs; ~59% of transported ^{3}H-Ch was found in HDFs of the BL medium of the apoAI-treated, Ctrlsi-transfected MAEC monolayer (Fig. 5D). The data in Fig. 5D also show that the HDF/total ^{3}H-Ch ratio in the BL medium of the vehicle-treated, ABCsi-transfected MAEC monolayer was ~35%, which is comparable with that of the vehicle-treated, Ctrlsi-transfected MAEC monolayer. This suggests that knockdown of ABCA1 did not affect the density distribution of the transendothelially transported ^{3}H-Ch under vehicle treatment conditions. In contrast, knockdown of ABCA1 attenuated the redistribution effect of apoAI on transendothelially transported ^{3}H-Ch. Specifically, only ~45% of the ^{3}H-Ch that had passed through the apoAI-treated, ABCsi-transfected MAEC monolayer was found in HDFs of the BL medium (Fig. 5D). This is significantly less than the HDF/total ^{3}H-Ch ratio in the BL medium of the apoAI-treated, Ctrlsi-transfected MAEC monolayer and is not significantly greater than the HDF/total ^{3}H-Ch ratio in the BL medium of the vehicle-treated, ABCsi-transfected MAEC monolayers.

Discussion/Conclusion

Binding of apoB-LPs to the cell membrane is an initial step for endocytosis and transcytosis of these lipoproteins. Data from the current report demonstrated that treatment of MAECs with apoAI slowed down apoB-LP uptake and transcellular transport but did not significantly reduce its binding to endothelial cells. This suggests that mechanisms other than inhibiting endothelial cell binding of apoB-LPs contribute to the diminished uptake and transendothelial transport of these lipoproteins. It has been reported that apoB-LPs pass through endothelial cells via a caveolae-mediated pathway involving SR-BI [5] and ALK1 [6]. Data from the current report show that apoAI treatment did not change the protein level of these caveolae-located receptors in MAECs but reduced their distribution in the raft membrane. These observations are consistent with our previous report showing that a substantial portion of caveolin-1 and raft cholesterol was allotted from the raft to the non-raft membrane fractions after MAECs were treated with apoAI [23]. Caveolins are a family of integral membrane proteins involved in caveolae formation in the plasma membrane [31]. Decrease in caveolins in the raft membrane likely expands the non-raft membrane area and reduces the number of caveolae in the plasma membrane, shifting caveolae-located receptors to the non-raft microdomain. Formation of ligand-receptor complexes in caveolae has been considered an initial step of caveolar endocytosis [31]. Thus, relocation of ALK1 and SR-BI

to the non-raft area of the plasma membrane may be a mechanism whereby apoAI inhibits endothelial cell uptake and transcytosis of apoB-LPs.

We also reported previously that the percentage of caveolin-1 and cholesterol in the raft membrane is related negatively to the level of total ABCA1 in MAECs, and knockdown of ABCA1 attenuates apoAI-induced relocation of caveolin-1 and raft cholesterol to the non-raft domains [23]. Data from the current study demonstrated that knockdown of ABCA1 also reduces the percentage of SR-BI and ALK1 in the raft membrane of MAECs treated with or without apoAI. These findings contribute to the notion that upregulation of ABCA1 expression is a mechanism for apoAI-induced relocation of raft-located proteins and lipids to the non-raft domains [23]. The membrane microdomain reorganization activity of ABCA1 also has been evidenced in other cell types [22]. However, the way in which ABCA1 distributes raft proteins and lipids to the non-raft area is poorly understood. One postulation attributes this to the lipid transporter activity of ABCA1. Specifically, ABCA1 functions as a ferry to convey phospholipids and unesterified cholesterol from the Golgi to the cell membrane [32]. The addition of these lipids to the plasma membrane results in a flop of lipids from the inner to the outer membrane leaflet, leading to microdomain lipid and protein redistribution [33].

Another important finding from the current study is that apoAI facilitates formation of apoE-carrying HDL-like particles during the AP-to-BL transport of apoB-LPs through the endothelial cell monolayer. Specifically, we observed that a portion of apoE and cholesterol of the apoB-LPs that passed through the MAEC monolayer presented in the HDFs of the BL medium. Treatment of the MAEC monolayer with apoAI significantly augmented the percentage of apoE and cholesterol in the HDFs. Similar to the observation in MAECs, transport of apoB-LPs through the HCAEC monolayer also forms apoE-carrying HDL-like particles. ApoAI inhibits transendothelial apoB-LP transport and enhances its associated HDL-like particle formation in HCAECs. These findings suggest that formation of apoE-carrying HDL-like particles is a common activity of mouse and human endothelial cells. Human apoB-LPs could serve as an efficient reagent to induce apoE-carrying HDL-like particle formation, regardless of the endothelial cells from mice or human subjects.

Besides the beneficial activity in endothelial cells, apoAI has been reported to promote apoE-carrying HDL-like particle formation in other cell types [13]. The promotive effect of apoAI on apoE-carrying HDL-like particle formation has been thought to be related to a mechanism involving ABCA1 [13]. Specifically, it has been suggested that interaction of apoAI with ABCA1 on the cell surface initiates an endocytosis of the apoAI–ABCA1 complex. The internalized apoAI travels to the sorting endosomes carrying endocytosed apoB-LPs, where apoAI facilitates the dissociation of apoE and lipids from the apoB-LP core and promotes apoE-carrying HDL-like particle formation and secretion [13]. The role of ABCA1 in endothelial cell uptake and transcytosis of apoAI has been demonstrated previously. Knockdown of ABCA1 has been shown to diminish endothelial cell binding, endocytosis, and transcytosis of apoAI [30]. The current report demonstrates that apoAI upregulates ABCA1 expression in MAECs, and knockdown of ABCA1 significantly reduces the percentage of cholesterol in HDFs of the BL medium of the apoAI-treated MAEC

monolayer. This provides direct evidence for the involvement of ABCA1 in the promotive activity of apoAI on apoE-carrying HDL-like particle formation in endothelial cells.

The current report for the first time demonstrated that apoAI inhibits transendothelial apoB-LP transport and promotes its associated apoE-carrying HDL-like particle formation via an ABCA1-dependent manner. In addition, we observed that apoAI promotes MAEC re-secretion of apoB-LPs and diminishes their accumulation in MAECs. Such information contributes to further understanding the mechanisms underlying the antiatherogenic activities of apoAI, and provides a theoretic foundation for developing targeted apoAI delivery to endothelial cells, especially the endothelial cells in the atherosclerotic area, for treatment of atherosclerosis-related cardiovascular diseases.

Acknowledgement

The authors would like to thank the Meharry Office of Scientific Editing and Publications for editorial assistance provided during manuscript preparation.

Funding sources

This study was supported by NIH grants SC1HL101431, G12 MD007586, U54MD0007593, and U54MD007586.

Data availability statement

All data supporting the findings of this study are available within the paper.

References

1. Tarbell JM: Mass transport in arteries and the localization of atherosclerosis. Annu Rev Biomed Eng 2003, 5:79–118. [PubMed: 12651738]
2. Pavlides S, Gutierrez-Pajares JL, Iturrieta J, Lisanti MP, Frank PG: Endothelial caveolin-1 plays a major role in the development of atherosclerosis. Cell Tissue Res 2014, 356(1):147–157. [PubMed: 24390341]
3. Frank PG, Pavlides S, Cheung MW, Daumer K, Lisanti MP: Role of caveolin-1 in the regulation of lipoprotein metabolism. Am J Physiol Cell Physiol 2008, 295(1):C242–248. [PubMed: 18508910]
4. Frank PG, Lee H, Park DS, Tandon NN, Scherer PE, Lisanti MP: Genetic ablation of caveolin-1 confers protection against atherosclerosis. Arterioscler Thromb Vasc Biol 2004, 24(1):98–105. [PubMed: 14563650]
5. Armstrong SM, Sugiyama MG, Fung KY, Gao Y, Wang C, Levy AS, Azizi P, Roufaiel M, Zhu SN, Neculai D et al. : A novel assay uncovers an unexpected role for SR-BI in LDL transcytosis. Cardiovasc Res 2015, 108(2):268–277. [PubMed: 26334034]
6. Kraehling JR, Chidlow JH, Rajagopal C, Sugiyama MG, Fowler JW, Lee MY, Zhang X, Ramirez CM, Park EJ, Tao B et al. : Genome-wide RNAi screen reveals ALK1 mediates LDL uptake and transcytosis in endothelial cells. Nat Commun 2016, 7:13516. [PubMed: 27869117]
7. He K, Yan X, Li N, Dang S, Xu L, Zhao B, Li Z, Lv Z, Fang X, Zhang Y et al. : Internalization of the TGF-beta type I receptor into caveolin-1 and EEA1 double-positive early endosomes. Cell Res 2015, 25(6):738–752. [PubMed: 25998683]
8. Yang H, Zhang N, Okoro EU, Guo Z: Transport of Apolipoprotein B-Containing Lipoproteins through Endothelial Cells Is Associated with Apolipoprotein E-Carrying HDL-Like Particle Formation. Int J Mol Sci 2018, 19(11):3593–3606. [PubMed: 30441770]
9. Farkas MH, Swift LL, Hasty AH, Linton MF, Fazio S: The recycling of apolipoprotein E in primary cultures of mouse hepatocytes. Evidence for a physiologic connection to high density lipoprotein metabolism. J Biol Chem 2003, 278(11):9412–9417. [PubMed: 12524433]

10. Hasty AH, Plummer MR, Weisgraber KH, Linton MF, Fazio S, Swift LL: The recycling of apolipoprotein E in macrophages: influence of HDL and apolipoprotein A-I. J Lipid Res 2005, 46(7):1433–1439. [PubMed: 15805547]
11. Heeren J, Grewal T, Jackle S, Beisiegel U: Recycling of apolipoprotein E and lipoprotein lipase through endosomal compartments in vivo. JBiolChem 2001, 276(45):42333–42338.
12. Heeren J, Grewal T, Laatsch A, Becker N, Rinninger F, Rye KA, Beisiegel U: Impaired recycling of apolipoprotein E4 is associated with intracellular cholesterol accumulation. J Biol Chem 2004, 279(53):55483–55492. [PubMed: 15485881]
13. Heeren J, Beisiegel U, Grewal T: Apolipoprotein E recycling: implications for dyslipidemia and atherosclerosis. Arterioscler Thromb Vasc Biol 2006, 26(3):442–448. [PubMed: 16373604]
14. Miyazaki O, Ogihara J, Fukamachi I, Kasumi T: Evidence for the presence of lipid-free monomolecular apolipoprotein A-1 in plasma. J Lipid Res 2014, 55(2):214–225. [PubMed: 24304668]
15. Lee-Rueckert M, Kovanen PT: Mast cell proteases: physiological tools to study functional significance of high density lipoproteins in the initiation of reverse cholesterol transport. Atherosclerosis 2006, 189(1):8–18. [PubMed: 16530202]
16. Rohrer L, Cavelier C, Fuchs S, Schluter MA, Volker W, von Eckardstein A: Binding, internalization and transport of apolipoprotein A-I by vascular endothelial cells. Biochim Biophys Acta 2006, 1761(2):186–194. [PubMed: 16546443]
17. Oram JF, Lawn RM, Garvin MR, Wade DP: ABCA1 is the cAMP-inducible apolipoprotein receptor that mediates cholesterol secretion from macrophages. J Biol Chem 2000, 275(44):34508–34511. [PubMed: 10918070]
18. Roosbeek S, Peelman F, Verhee A, Labeur C, Caster H, Lensink MF, Cirulli C, Grooten J, Cochet C, Vandekerckhove J et al. : Phosphorylation by protein kinase CK2 modulates the activity of the ATP binding cassette A1 transporter. J Biol Chem 2004, 279(36):37779–37788. [PubMed: 15218032]
19. Takahashi Y, Smith JD: Cholesterol efflux to apolipoprotein AI involves endocytosis and resecretion in a calcium-dependent pathway. Proc Natl Acad Sci U S A 1999, 96(20):11358–11363. [PubMed: 10500181]
20. Wang N, Chen W, Linsel-Nitschke P, Martinez LO, Agerholm-Larsen B, Silver DL, Tall AR: A PEST sequence in ABCA1 regulates degradation by calpain protease and stabilization of ABCA1 by apoA-I. J Clin Invest 2003, 111(1):99–107. [PubMed: 12511593]
21. Mendez AJ, Lin G, Wade DP, Lawn RM, Oram JF: Membrane lipid domains distinct from cholesterol/sphingomyelin-rich rafts are involved in the ABCA1-mediated lipid secretory pathway. J Biol Chem 2001, 276(5):3158–3166. [PubMed: 11073951]
22. Landry YD, Denis M, Nandi S, Bell S, Vaughan AM, Zha X: ATP-binding cassette transporter A1 expression disrupts raft membrane microdomains through its ATPase-related functions. J Biol Chem 2006, 281(47):36091–36101. [PubMed: 16984907]
23. Yang H, Zhang N, Guo ZM: Redistribution of membrane raft microdomains by apolipoprotein A-I in mouse aortic endothelial cells. Cardiovasc Dis Med 2020, 1(1):2–6.
24. Barter PJ, Jones ME: Kinetic studies of the transfer of esterified cholesterol between human plasma low and high density lipoproteins. J Lipid Res 1980, 21(2):238–249. [PubMed: 7373163]
25. Wu DF, Sharan C, Yang H, Goodwin JS, Zhou L, Grabowski GA, Du H, Guo ZM: Apolipoprotein E-deficient lipoproteins induce foam cell formation by downregulation of lysosomal hydrolases in macrophages. JLipid Res 2007, 48:2571–2578. [PubMed: 17720994]
26. Guo ZM, Van Remmen H, Yang H, Chen XL, Mele J, Vijg J, Epstein CJ, Ho Y-S, Richardson A: Changes in expression of antioxidant enzymes affect cell-mediated LDL oxidation and oxLDL-induced apoptosis in mouse aorta cells. ArteriosclerThrombVascBiol 2001, 21:1131–1138.
27. Chapman MJ, Goldstein S, Lagrange D, Laplaud PM: A density gradient ultracentrifugal procedure for the isolation of the major lipoprotein classes from human serum. J Lipid Res 1981, 22(2):339–358. [PubMed: 6787159]
28. Macdonald JL, Pike LJ: A simplified method for the preparation of detergent-free lipid rafts. J Lipid Res 2005, 46(5):1061–1067. [PubMed: 15722565]

29. Lin X, Yang H, Zhang H, Zhou L, Guo Z: A novel transcription mechanism activated by ethanol: induction of Slc7a11 gene expression via inhibition of the DNA-binding activity of transcriptional repressor octamer-binding transcription factor 1 (OCT-1). JBiolChem 2013, 288(21):14815–14823.

30. Cavelier C, Rohrer L, von Eckardstein A: ATP-Binding cassette transporter A1 modulates apolipoprotein A-I transcytosis through aortic endothelial cells. Circ Res 2006, 99(10):1060–1066. [PubMed: 17053191]

31. Parton RG, Richards AA: Lipid rafts and caveolae as portals for endocytosis: new insights and common mechanisms. Traffic 2003, 4(11):724–738. [PubMed: 14617356]

32. Phillips MC: Is ABCA1 a lipid transfer protein? J Lipid Res 2018, 59(5):749–763. [PubMed: 29305383]

33. Nagao K, Tomioka M, Ueda K: Function and regulation of ABCA1--membrane meso-domain organization and reorganization. FEBS J 2011, 278(18):3190–3203. [PubMed: 21554545]

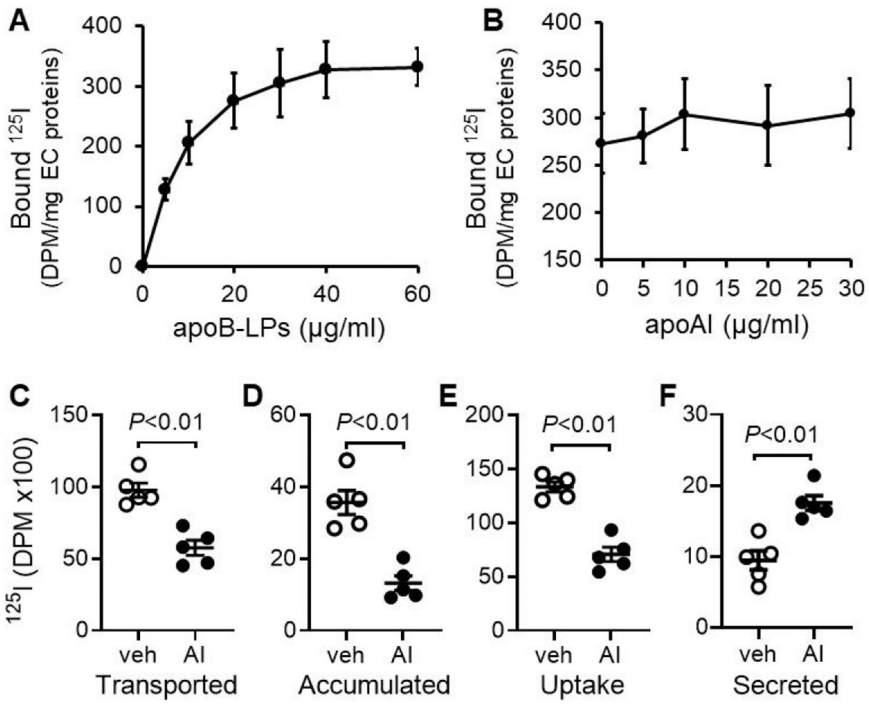

Fig. 1.

The effect of apoAI on MAEC binding, uptake, and transcellular transport of apoB-LPs. **A:** MAECs grown in a 12-Well culture plate were incubated sequentially in OptiMEM™ medium on ice for 30 min and indicated doses of ^{125}I-labeled apoB-LPs on ice for 30 min. **B:** MAECs grown in a 12-Well culture plate were pretreated with 0 μg/ml to 30 μg/ml of apoAI at 37°C for 4 h and then incubated with 20 μg/ml of ^{125}I-labeled apoB-LPs on ice for 30 min. **A–B:** Lipoproteins bound to the cell were determined by cell-associated radioactivity. **C-E:** The AP side of the MAEC monolayer grown on a Transwell™ membrane was treated with 20 μg/ml of ^{125}I-labeled apoB-LPs in the presence of 20 μg/ml apoAI (AI) or vehicle medium (veh), and the BL side was treated with medium alone for 24 h. Lipoproteins transported through the MAEC monolayer were determined by radioactivity in the BL medium. Lipoproteins accumulated in MAECs were determined by radioactivity in the cells. Lipoproteins taken up (uptake) by MAECs were determined by the sum of radioactivity in the BL medium and radioactivity in cells. **F:** The MAEC monolayer, treated with apoB-LPs ± apoAI as above, was washed with low ionic strength solution and then incubated with fresh medium for another 24 h. Lipoproteins secreted from MAECs were determined by the sum of radioactivity in the AP and BL media. Values represent the mean ± SE of five experiments. The difference between vehicle- and apoAI-treated cells was analyzed by student's t-test.

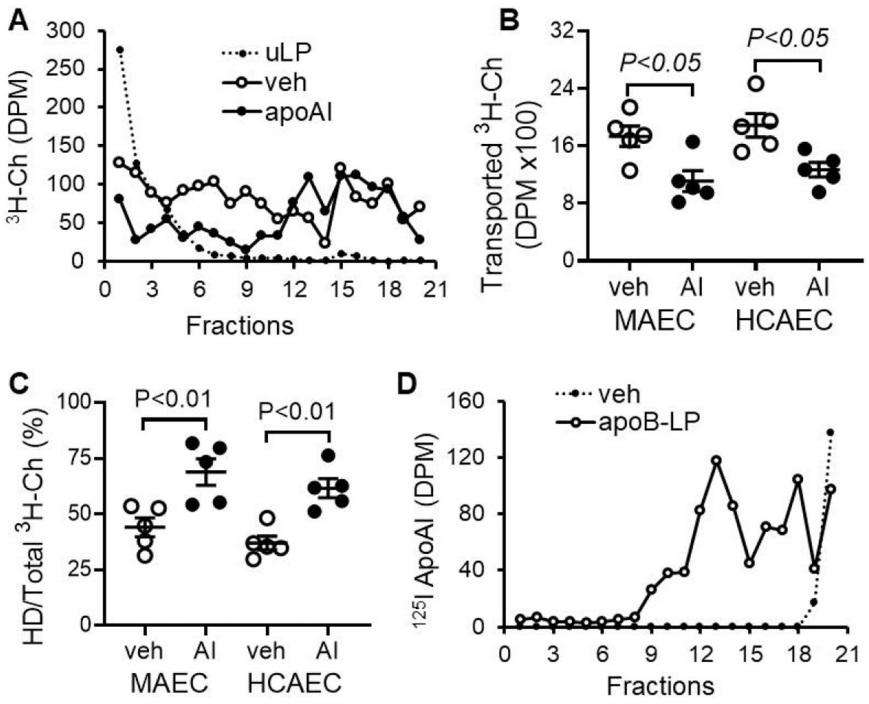

Fig. 2.

The effect of apoAI on formation of HDL-like particles in MAECs and HAECs. **A–C:** The AP side of the MAEC or HCAEC monolayer grown on a Transwell™ membrane was incubated with 20 μg/ml of ^{3}H-Ch-labeled apoB-LPs in the presence of 20 μg/ml of unlabeled apoAI (AI) or vehicle medium (veh). The BL side was incubated with medium alone for 24 h. As a control, 0.4 μg/ml of ^{3}H-Ch-labeled apoB-LPs was incubated with medium in the absence of cells at 37°C for 24 h. The BL media and cell-untreated ^{3}H-Ch-labeled apoB-LPs (uLP) were subjected to discontinuous gradient ultracentrifugation. Twenty fractions were collected for determination of radioactivity. Panel **A** shows representative density curves of the radioactivity in the cell-untreated apoB-LPs and the BL medium of the MAEC monolayer. The amount of ^{3}H-Ch transported through the MAEC and HCAEC monolayer was determined by the sum of radioactivity in all fractions of the BL medium **(B).** The ^{3}H-Ch level in the HDFs of the BL media of the MAEC and HCAEC monolayer was expressed as the % of HDF ^{3}H-Ch in the total ^{3}H-Ch (HD / total ^{3}H-Ch) **(C)**, which was calculated as follows: (radioactivity in fractions ten through twenty / radioactivity in fractions one through twenty) x100. Values represent the mean ± SE of four experiments. The difference between vehicle- and apoAI-treated cells was analyzed by student's t test. **D:** The AP side of the MAEC monolayer grown on a Transwell™2 membrane was incubated with 0.2 μg/ml of ^{125}I-apoAI in the presence of 20 μg/ml of unlabeled apoB-LPs or veh. The BL side was incubated with medium alone for 24 h. The BL media were subjected to discontinuous gradient ultracentrifugation. Twenty fractions were collected for determination of radioactivity.

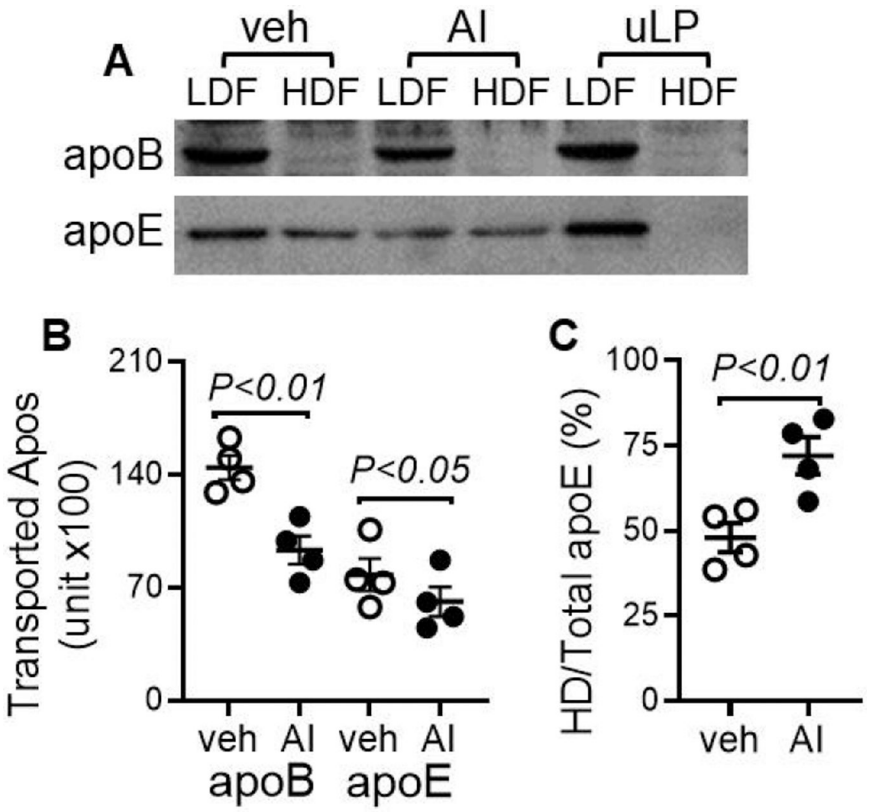

Fig. 3.

The effect of apoAI on transport of apoB-LP-associated apolipoproteins through the MAEC monolayer. The AP side of the MAEC monolayer was incubated with 20 μg/ml unlabeled apoB-LPs (uLP) in the presence of 20 μg/ml apoAI (AI) or vehicle medium (veh), and the BL side was incubated with medium alone for 24 h. The BL medium of the MAEC monolayer and 10 μg of cell-untreated apoB-LPs were subjected to discontinuous gradient ultracentrifugation. Proteins in the LDF and HDF were subjected to WB analysis of apoB and apoE **(A)**. The amount of apoB and apoE transported through the endothelial cell monolayer was determined as the sum of the immunoreactive intensity of the BL medium's LDF and HDF **(B).** The % of apoE in the HDF to the total apoE (HDF /total apoE) in the BL media was calculated as follows: [apoE in the HDF / (apoE in the HDF + apoE in the LDF)] x100 **(C)**. Values represent the mean ± SE of four experiments. The difference between vehicle- and apoAI-treated cells was analyzed by student's t test.

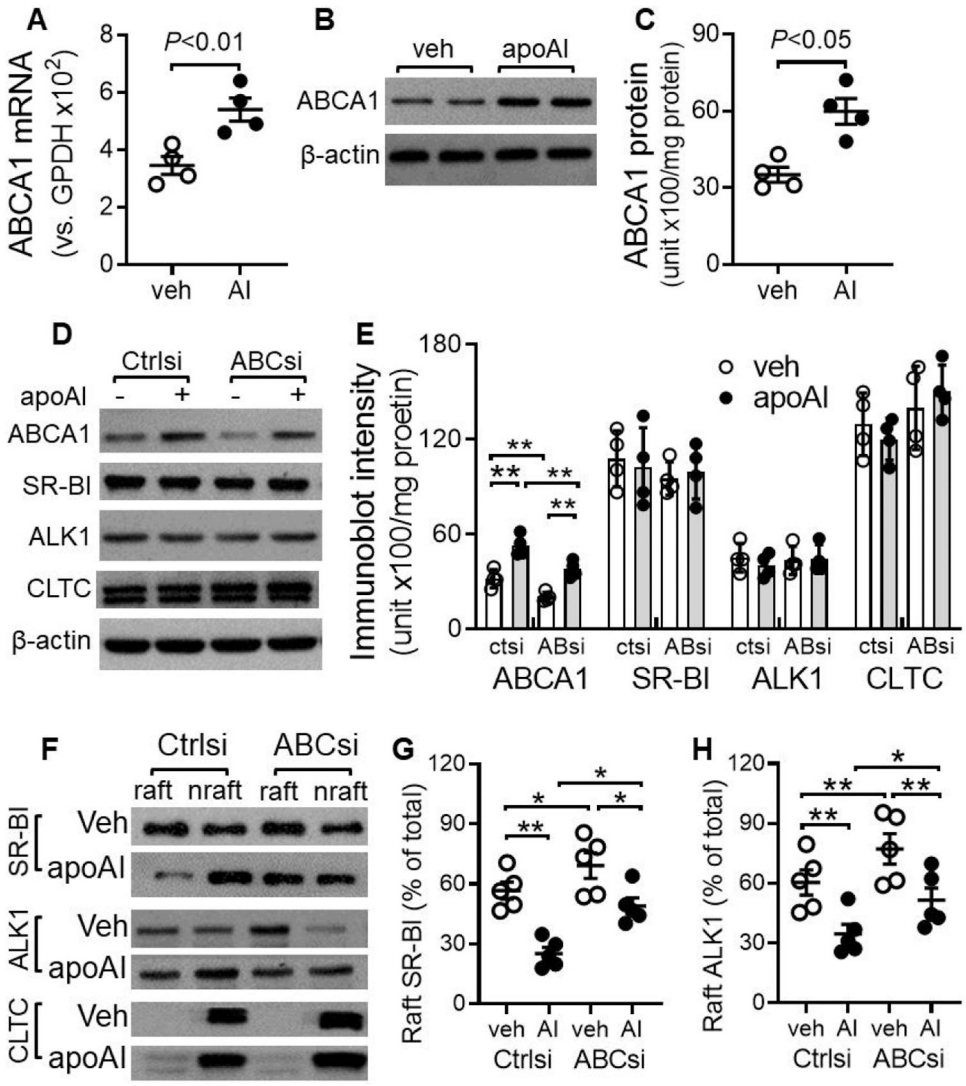

Fig. 4.

The effect of apoAI on ABCA1 expression, and the effect of apoAI treatment and ABCA1 knockdown on the distribution of SR-BI and ALK1 in membrane microdomains. **A–C:** MAECs grown in 6-Well plates were incubated with vehicle medium (veh) or 20μg/ml of apoAI (AI) at 37°C for 4 h. The ABCA1 mRNA level was determined by quantitative real-time RT-PCR and expressed relative to GAPDH mRNA **(A).** The ABCA1 protein level was determined by WB analysis, and normalized as immunoreactive intensity units/mg endothelial cell proteins. Values represent the mean ± SE of four experiments. Data were analyzed by Student's *t*-test **(B-C). D–G:** MAECs grown on a Transwell™ membrane were transfected with ABCsi or scrambled Ctrlsi. The AP side of the MAEC monolayer was incubated with 20 μg/ml of apoAI or vehicle medium; the BL side was incubated with medium alone at 37°C for 16 h. The protein level of ABCA1, SR-BI, ALK1, and CLTC was determined by WB analysis, and normalized as immunoreactive intensity units/mg endothelial cell proteins **(D–E)**. Treated MAECs were collected and homogenized by passage through a syringe needle. The postnuclear extracts were subjected to a 10 ml

OptiPrep™ gradient ultracentrifugation. The raft and non-raft fractions of the gradient were collected separately and subjected to WB analysis of SR-BI, ALK1, and CLTC **(F).** The percentage of SR-BI **(G)** and ALK1 **(H)** in the raft fraction was calculated as follows: (the immunoreactive intensity of the raft fraction / the sum of the immunoreactive intensity of raft and non-raft fractions) x 100. Values represent the mean ± SE of four experiments. Data were analyzed by one-way analysis of variance, followed by Tukey's post-hoc test. *$P <$ 0.05 and ** $P < 0.01$ between the indicated groups.

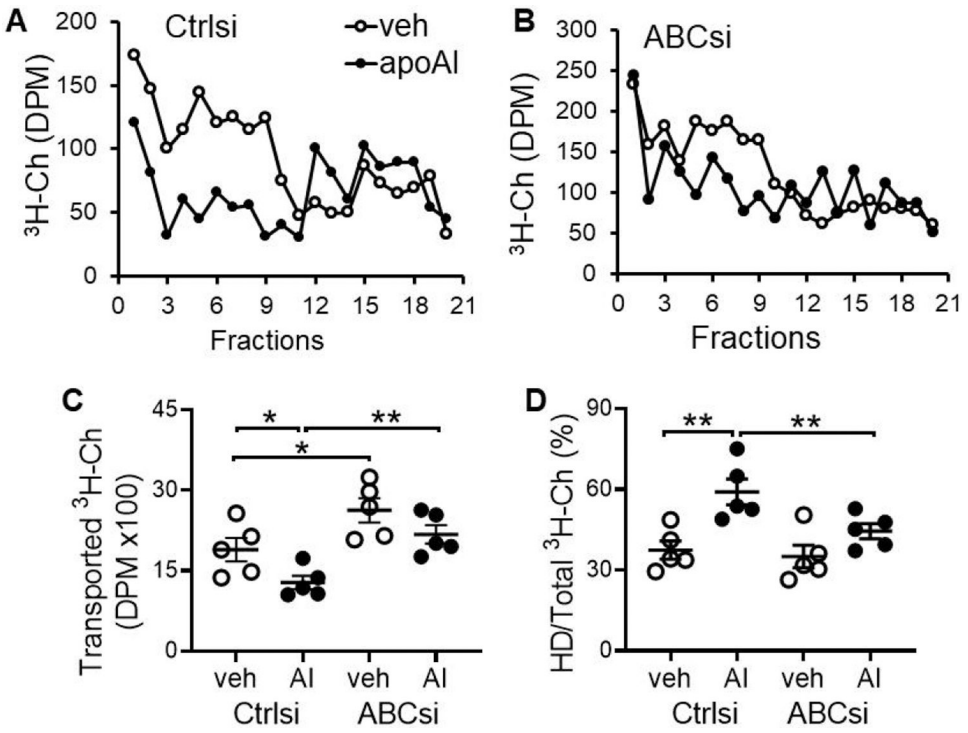

Fig. 5.

The effect of apoAI treatment and ABCA1 knockdown on transendothelial transport of apoB-LPs and its associated HDL-like particle formation. **A–B:** MAECs grown on a Transwell™ membrane were transfected with scrambled Ctrlsi **(A)** or ABCsi **(B).** The AP side of the MAEC monolayer was incubated with 20 μg/ml of ^{3}H-Ch-apoB-LPs in the presence of 20 μg/ml of apoAI (AI) or vehicle medium (veh); the BL side was incubated with medium alone for 24 h. The BL media were subjected to discontinuous gradient ultracentrifugation. Twenty fractions were collected for determination of radioactivity. **C:** The amount of ^{3}H-Ch transported through the MAEC monolayer was determined by the sum of radioactivity in all fractions of the BL medium. **D:** The ^{3}H-Ch level in the HDFs of the BL media was expressed as the % of HDF ^{3}H-Ch in the total ^{3}H-Ch (HD / total ^{3}H-Ch), which was calculated as follows: (the radioactivity in fractions ten through twenty / the radioactivity in fractions one through twenty) x100. Values represent the mean ± SE of five experiments. Data were analyzed by one-way analysis of variance, followed by Tukey's post-hoc test. *$P < 0.05$ and ** $P < 0.01$ between the indicated groups.